Supplementary information for:

Ultrafast spectroscopy of biliverdin dimethyl ester in solution: pathways of excited-state depopulation

Yangyi Liu[1], Zhuang Chen[1], Xueli Wang[1], Simin Cao[1], Jianhua Xu[1,2], Ralph Jimenez[3,4]*, and Jinquan Chen[1,2]*

1. State Key Laboratory of Precision Spectroscopy, East China Normal University, Shanghai, China

2. Collaborative Innovation Center of Extreme Optics, Shanxi University, Taiyuan, Shanxi 030006, China

3. JILA, NIST and University of Colorado, Boulder, USA

4. Department of Chemistry, University of Colorado, Boulder, CO USA.

Supplementary Figures

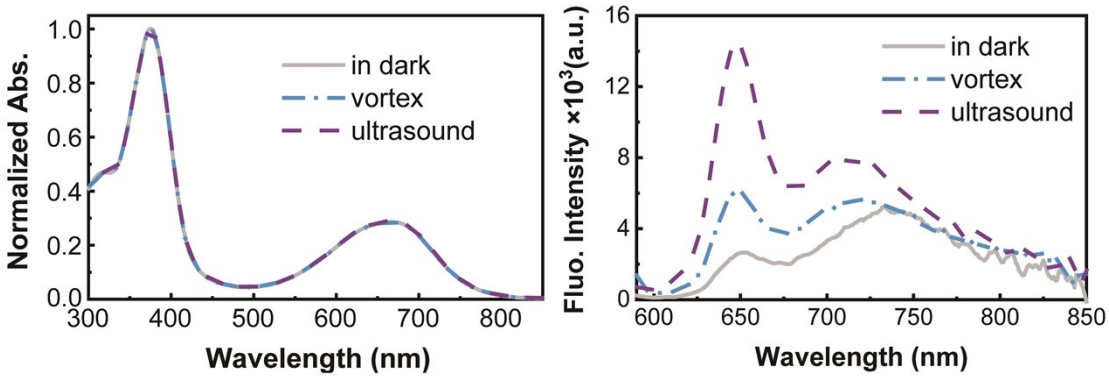

Figure S1. Absorption and fluorescence emission spectra of BVE in methanol.

(Further description are given in the next chapter)

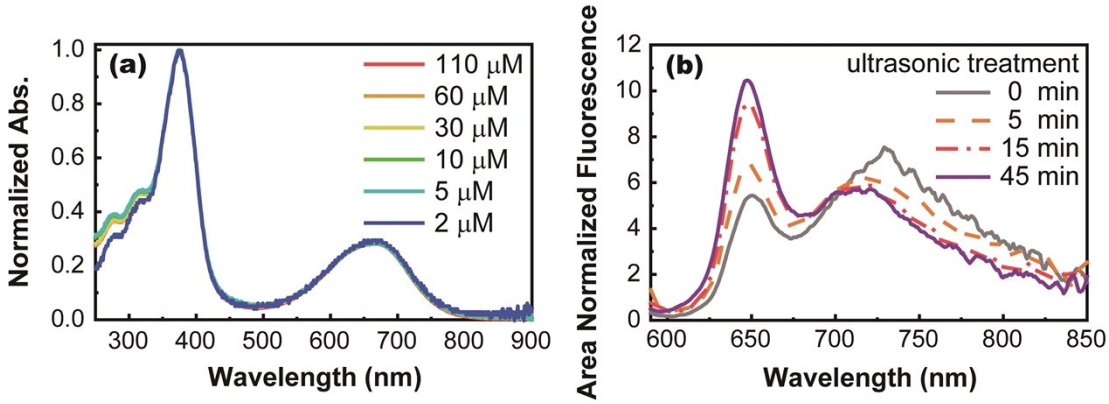

Figure S2. (a) Normalized absorption spectra of different concentrations of BVE in methanol. (b) Area normalized fluorescence emission spectra of BVE–methanol solution sonicated for various amounts of time.

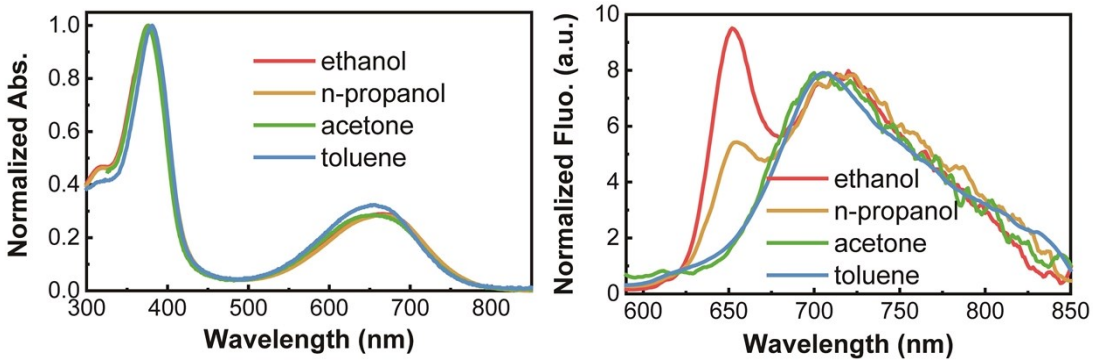

Figure S3. Absorption and fluorescence emission spectra of BVE in other solutions.

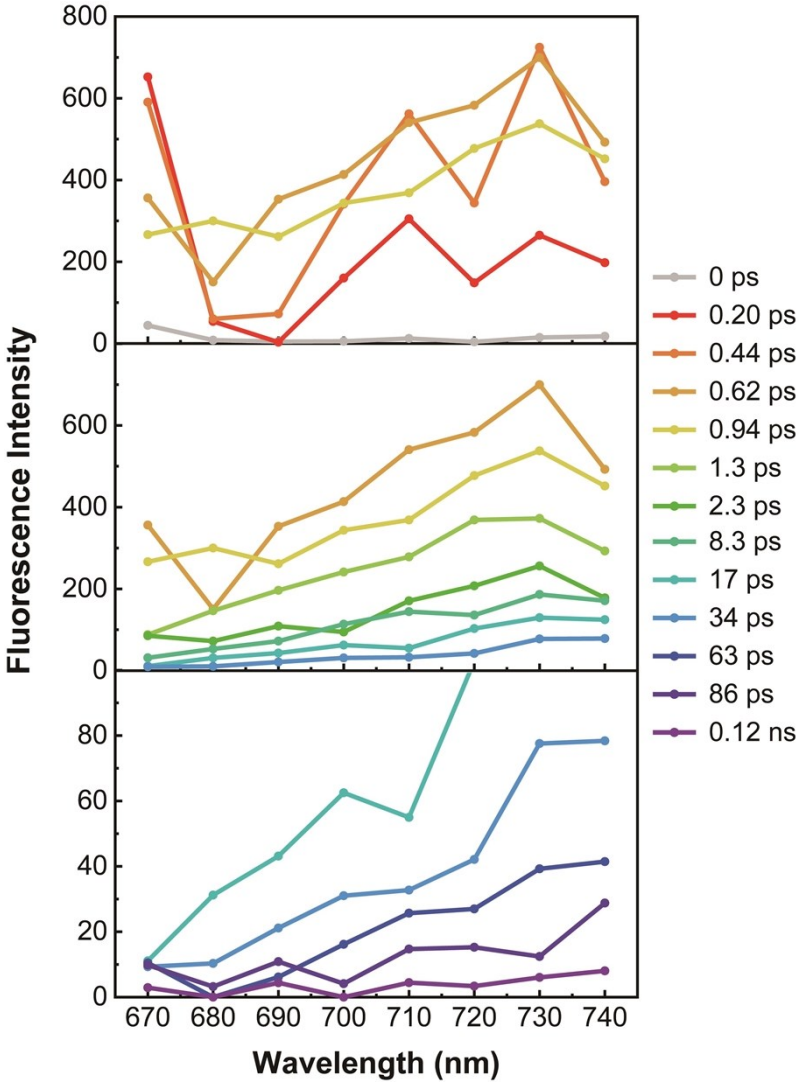

Figure S4. Fluorescence TRES from the up-conversion experiment.

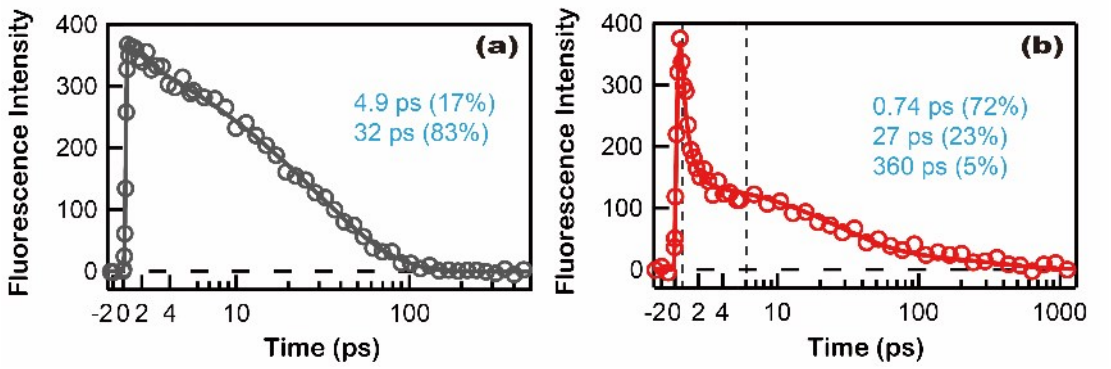

Figure S5. Representative fluorescence up-conversion kinetics of BVE in (a) $CHCl_3$ and (b) CH_3OH (630 nm excitation and 720 nm detection).

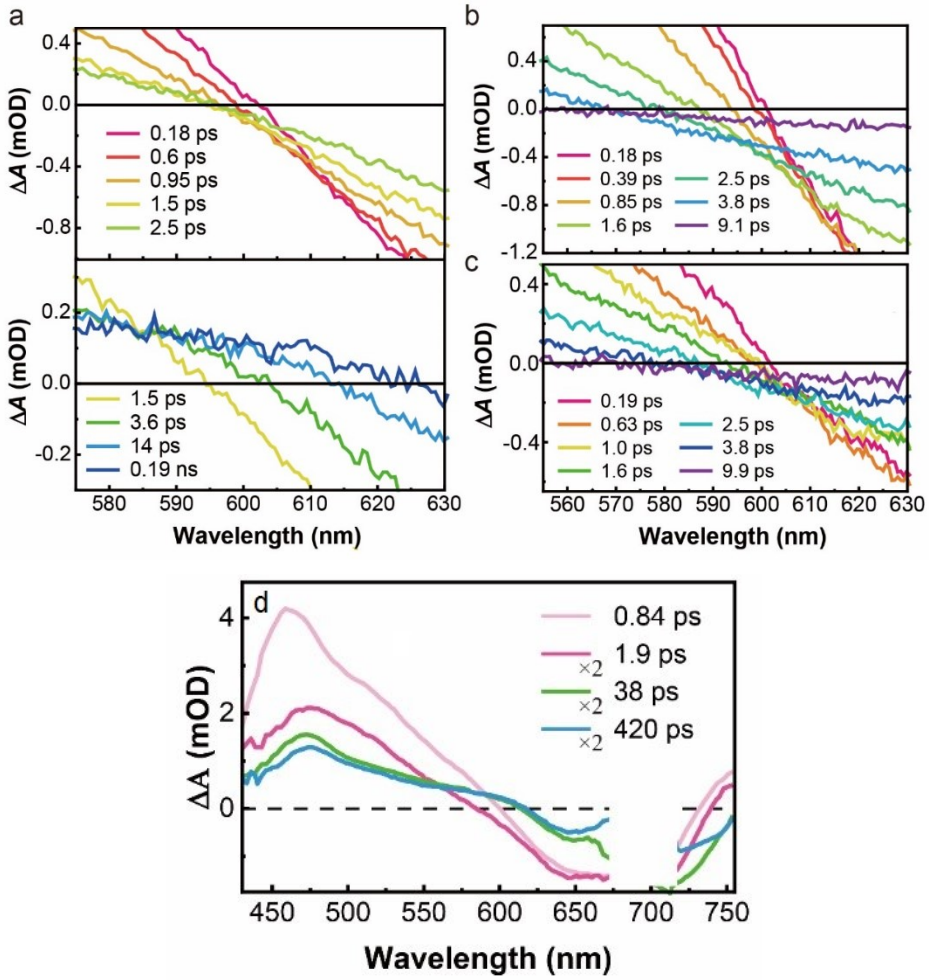

Figure S6. TA spectra shown in narrow range of coordinates for BVE in methanol (a), acetonitrile (b) and chloroform (c). EADS of BVE in methanol (d). The amplitudes for three of these components was scaled for better comparison.

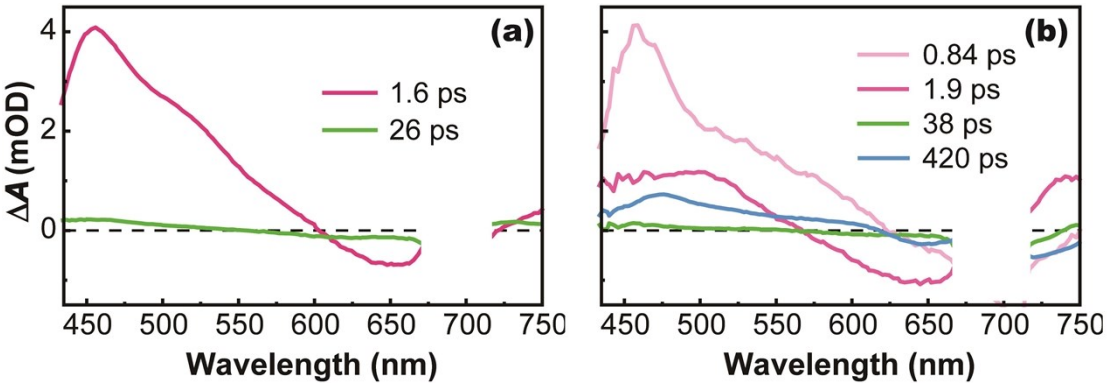

Figure S7. DAS of BVE in (a) chloroform and (b) methanol.

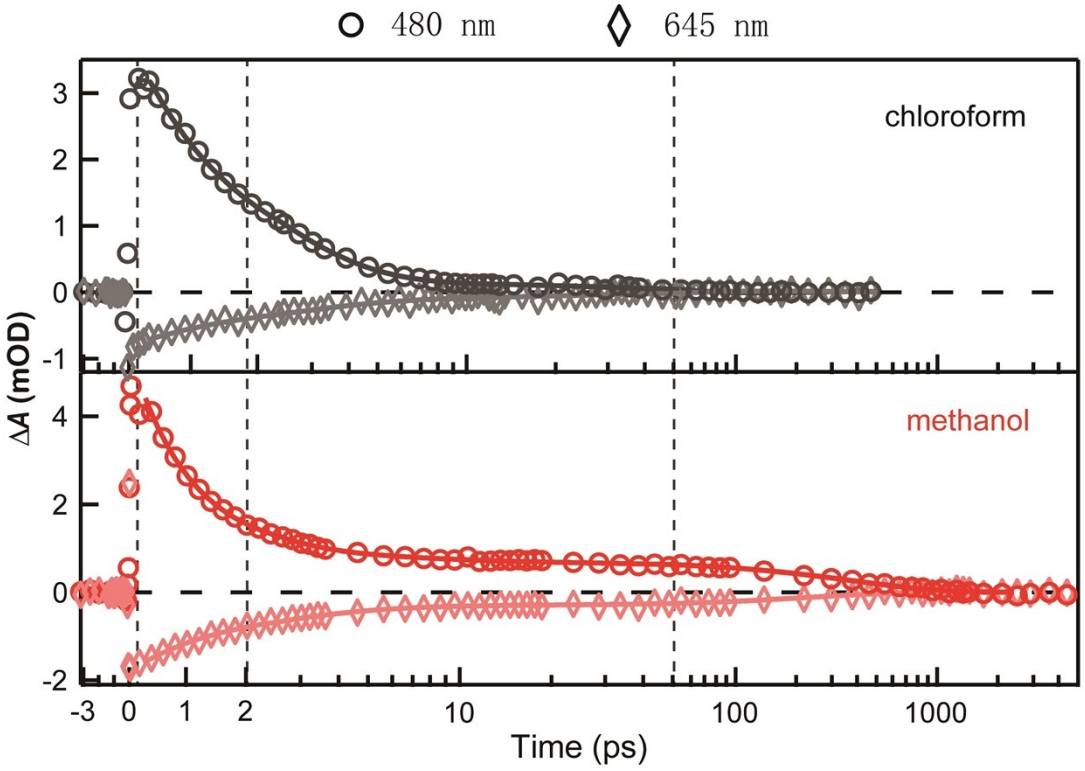

Figure S8. Kinetics for BVE in chloroform (grey) and methanol (red) Circles indicate probe at 480 nm and diamonds indicate probe at 645 nm).

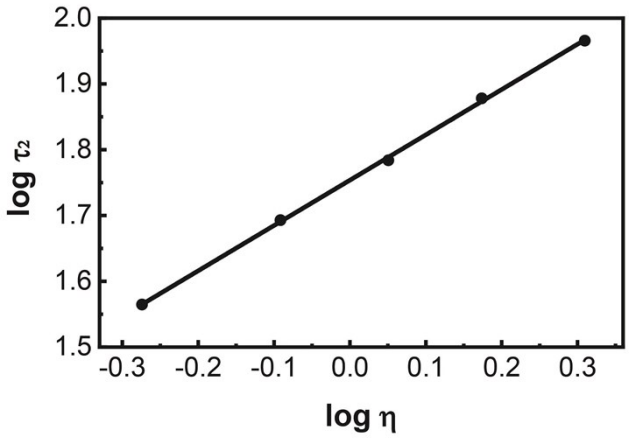

Figure S9. The changes in τ_2 for BVE in chloroform mixtures as a function of viscosity.

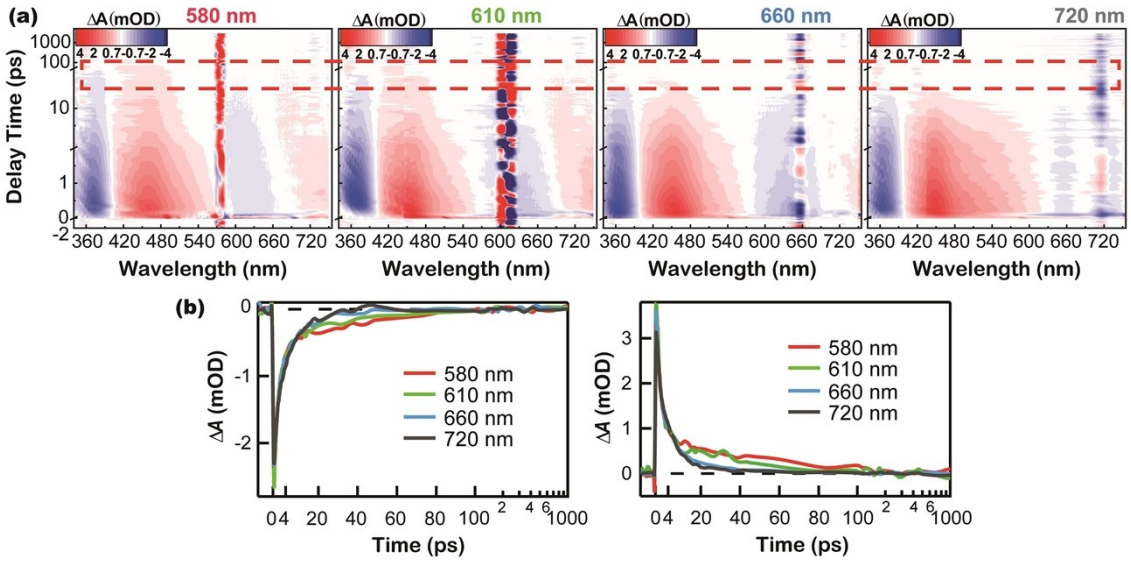

Figure S10. TA data of BVE in acetonitrile. (a) TA spectra of BVE in acetonitrile at the indicated pump wavelengths. The red dashed box shows the loss of the ~30 ps component as pump wavelength increases. (b) Kinetics for probe at 390 nm (left, for GSB signal) and 460 nm (right, for EAS signal).

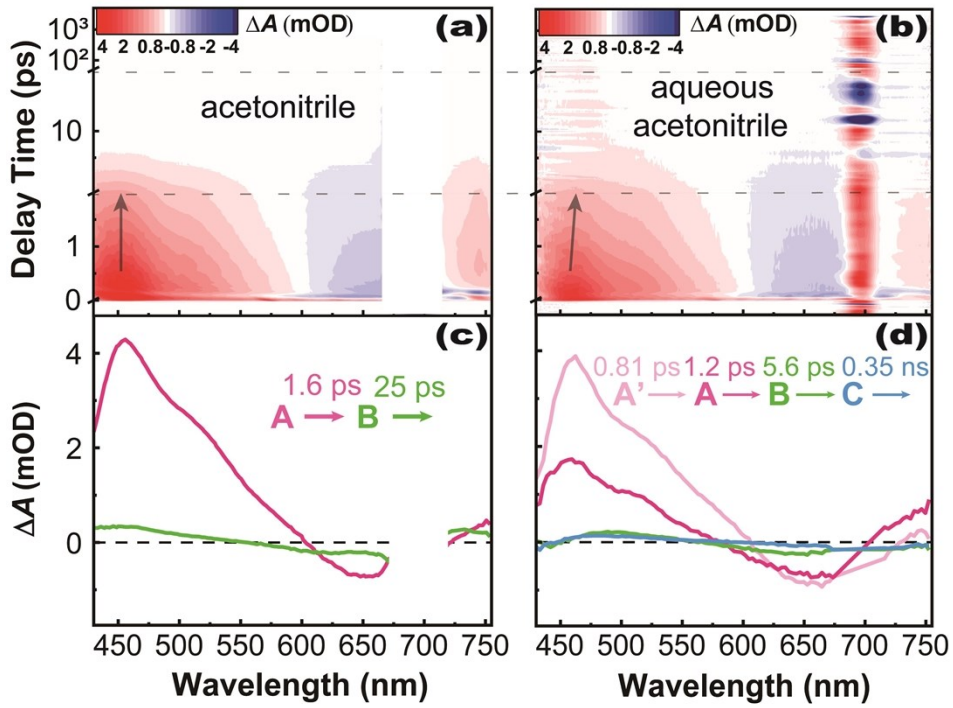

Figure S11. Broadband transient absorption spectra of BVE in (a) acetonitrile and (b) aqueous acetonitrile. Panel (c) and (d) are the corresponding EADS from global fitting for (a) and (b), respectively.

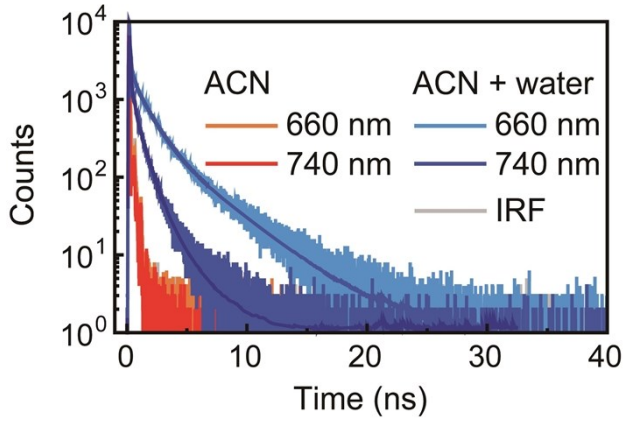

Figure S12. Time-resolved fluorescence decay spectra for BVE in acetonitrile and aqueous acetonitrile. The excitation wavelength is 580 nm.

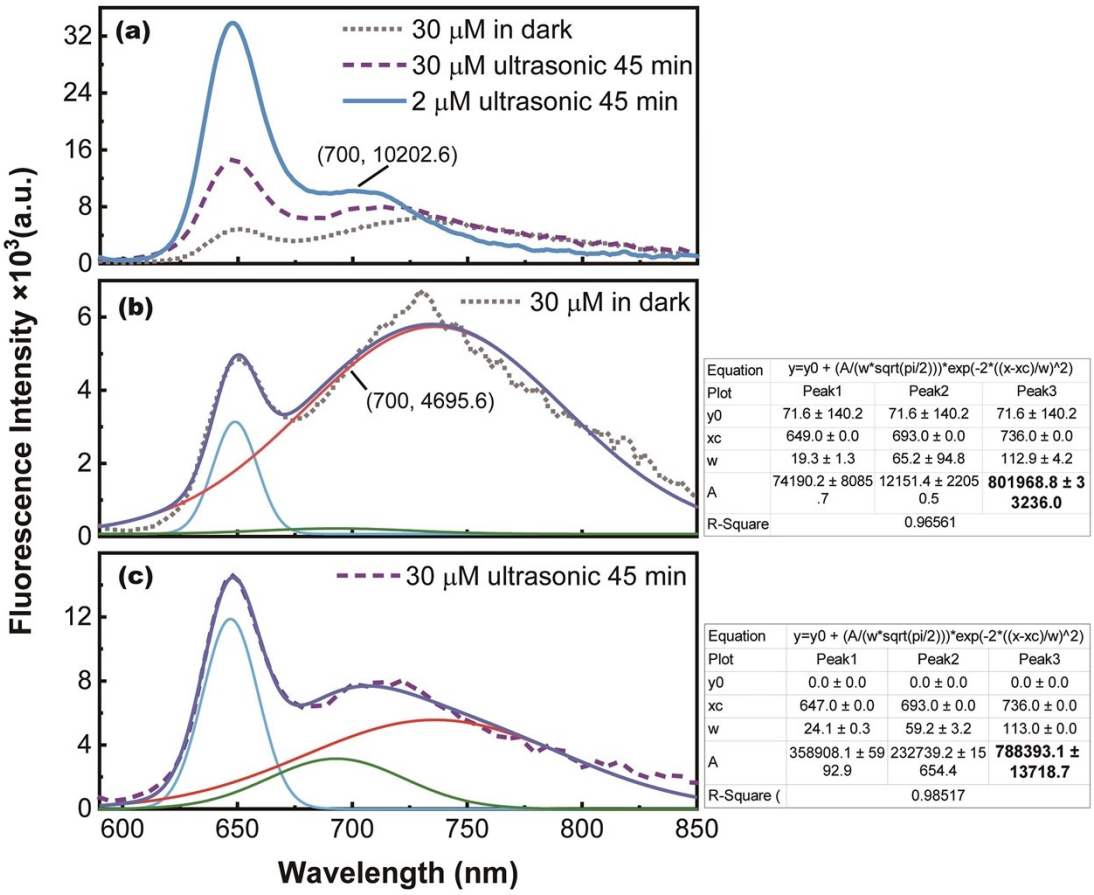

Equation	y=y0 + (A/(w*sqrt(pi/2)))*exp(-2*((x-xc)/w)^2)		
Plot	Peak1	Peak2	Peak3
y0	71.6 ± 140.2	71.6 ± 140.2	71.6 ± 140.2
xc	649.0 ± 0.0	693.0 ± 0.0	736.0 ± 0.0
w	19.3 ± 1.3	65.2 ± 94.8	112.9 ± 4.2
A	74190.2 ± 8085.7	12151.4 ± 22050.5	**801968.8 ± 33236.0**
R-Square	0.96561		

Equation	y=y0 + (A/(w*sqrt(pi/2)))*exp(-2*((x-xc)/w)^2)		
Plot	Peak1	Peak2	Peak3
y0	0.0 ± 0.0	0.0 ± 0.0	0.0 ± 0.0
xc	647.0 ± 0.0	693.0 ± 0.0	736.0 ± 0.0
w	24.1 ± 0.3	59.2 ± 3.2	113.0 ± 0.0
A	358908.1 ± 5992.9	232739.2 ± 15654.4	**788393.1 ± 13718.7**
R-Square (	0.98517		

Figure S13. Fluorescence emission spectra for BVE in CH_3OH. Results of multiple peak fits are shown in panels b and c. The detailed calculation of LBVE QY is given in the next chapter.

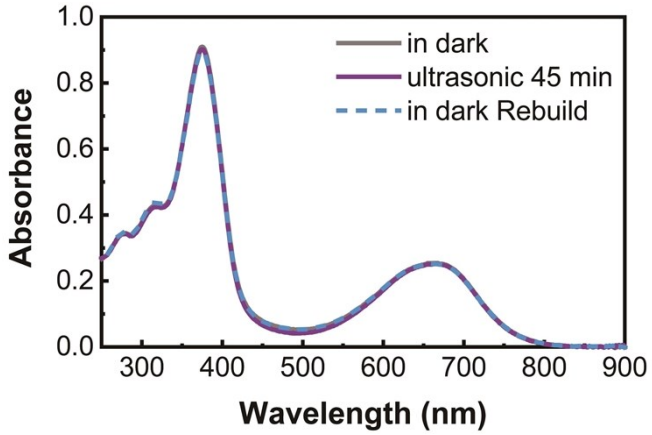

Figure S14. A reconstructed absorption spectrum (blue dashed line) compared with the original absorption (grey line) and the absorption spectrum after 45 min of

ultrasonic treatment (purple line).

Additional Results and Discussion

Description of Figure S1

The grey line is the control group (BVE dissolved in solvent and then placed in the dark for 15 min). The blue line is BVE solution vortexed for ~15 min. The purple line is BVE solution ulrasonicicated for ~15 min.

From the spectra we can see that there is no distinguishable difference between the absorption spectra of these three samples. However, the fluorescence emission was significantly different (especially after ultrasonic treatment). For the sonicated BVE solution, the increase in fluorescence intensity at 740 nm is caused by a shoulder band of the luminous component with a main peak at 650 nm. Therefore, traditional methods (such as vortexing, sonication and heating) used to help dissolve the sample should be avoided when prepared BVE solutions. With this in mind, all of the BVE solvent–solutions in this work were kept in dark for at least 15 min before any measurment.

Estimation of fluorescence quantum yield of LBVE

In a two species emission system, an isoemissive point would appear. The ratio of wavelength-dependent QY is equal to the ratio of the total QY of the emitting species in the solution at the isoemissive point.[1]

Namely,

$$\frac{\varphi_A}{\varphi_B} = \frac{\varphi_{A(\lambda)}}{\varphi_{B(\lambda)}}$$

In the case of the 2 μM BVE–methanol solution ultrasonicated for 45 mins (Figure S13a, blue line), most of its fluorescence emission comes from LBVE. The ratio of $\varphi_{A(\lambda = 700\,nm)}/\varphi_A$ is ~0.0054, which should be equal to the ratio in emission spectra of BVE, theoretically. The emission spectra can be fitted with three peaks as shown in Figure S13b and c. The blue and green lines are thought to be the emission components of LBVE, and the red line represents BVE. The ratio of $\varphi_{B(\lambda = 700\,nm)}/\varphi_B$ for the reconstructed BVE emission spectra is ~0.0058, which is very close to the value of LBVE above. This numerical agreement reflects the validity of our modeling parameters.

As shown in the inserted tables in Figure S13b and c, the integral area of the red peak (peak 3) decreased by about 1.7%. This change directly reflects the change in the fluorescence emission of BVE (at low concentrations, the emission intensity is linearly related to the concentration):

$$\Delta n_{BVE} \sim \Delta A_{f_{peak3}}$$

Under our experimental conditions (ultrasonication), no other BVE loss behavior was allowed to occur. Thus, we can conclude that 1.7% of the BVE turns into LBVE during the 45 min treatment and this leads to the increase of the total fluorescent emission integral area:

$$\Delta A_f = \Delta A_{f_{peak1}} + \Delta A_{f_{peak2}} + \Delta A_{f_{peak3}}$$

We show the equation for measuring fluorescence QY by the relative method below:

$$\varphi_f = \varphi_r \times \frac{I_s}{I_r} \times \frac{Abs_r}{Abs_s} \times \frac{{\eta_r}^2}{{\eta_s}^2}$$

Since only one solvent is involved, the refractive index can be eliminated in this experiment. The fluorescence QY of BVE was taken as φ_r. Therefore, we only need the change of absorbance at the excitation wavelength to deduce the fluorescence QY of LBVE.

It can reasonably be induced here that LBVE has an absorption extinction coefficient similar to that of BVE except that there is a blue shift of the entire spectrum. A similarly shaped excitation spectrum with the same blue shift strongly supports this assumption (Figure 2e). A simulated, reconstructed absorption spectrum was created by blue shifting the original BVE absorption spectrum of 1.7% intensity and then adding it to the original BVE spectrum of 98.3% intensity. As shown in Figure S14, the simulated reconstruction (blue dashed line) showed no obvious absorbance difference at the excitation wavelength (580 nm) from the original spectrum (grey line) or the experimental results (purple line). Therefore, under the conditions that the absorbance is basically unchanged, the ratio of the change of the fluorescence integral area can be approximated as the ratio of the fluorescence QY, that is:

$$\frac{\varphi_{f_{LBVE}}}{\varphi_{f_{BVE}}} \sim \frac{\Delta A_{f_{LBVE}}}{\Delta A_{f_{BVE}}}$$

Thus, the fluorescence QY of LBVE is 37 times that of BVE (0.01% in CH_3OH at room temperature).

Supplementary Tables

Table S1. Fitting result of TCSPC data for BVE and its treated solutions

	λ^{exc}/nm	λ^{em}/nm	τ_1/ns	□τ_2/ns	□τ_3/ns	□τ_4/ns
BVE in methanol	580	660	< 0.2 (75.9%)	-	0.7 ± 0.2 (6.4%)	4.6 ± 0.1 (17.6%)
		700	< 0.2 (93.6%)	-	0.7 ± 0.2 (4.5%)	4.6 ± 0.3 (1.9%)
		740	< 0.2 (93.7%)	0.5 ± 0.1 (5.2%)	-	4.4 ± 0.2 (1.1%)
		780	< 0.2 (94.6%)	0.5 ± 0.1 (4.8%)	-	4.6 ± 0.8 (0.6%)
BVE in methanol (after ultrasonication)	580	660	< 0.2 (69.5%)	-	1.4 ± 0.3 (7.5%)	4.7 ± 0.1 (23.0%)
		700	< 0.2 (92.6%)	-	1.0 ± 0.4 (4.6%)	4.7 ± 0.2 (2.8%)
		740	< 0.2 (87.7%)	0.5 ± 0.1 (10.8%)	-	4.4 ± 0.1 (1.5%)
		780	< 0.2 (91.2%)	0.5 ± 0.2 (8.1%)	-	4.5 ± 0.3 (0.7%)
	700	740	< 0.2 (24.4%)	0.4 ± 0.1 (75.6%)	-	-
		780	< 0.2 (31.4%)	0.4 ± 0.1 (68.6%)	-	-
BVE in acetonitrile water mixture	580	660	< 0.2 (73.6%)	-	1.2 ± 0.1 (20.0%)	3.8 ± 0.4 (6.4%)
		740	< 0.2 (81.6%)	0.6 ± 0.1 (17.2%)	-	2.2 ± 0.1 (1.2%)

Table S2. Best fitting for single wavelength fluorescence up-conversion kinetics at

720 nm of BVE in $CHCl_3$ and CH_3OH

	τ_1/ps	τ_2/ps	τ_3/ps	τ_4/ps
chloroform	-	4.9 ± 0.8 (17%)	32 ± 1 (83%)	-
methanol	0.74 ± 0.16 (72%)	-	27 ± 2 (23%)	360 ± 10 (5%)

Table S3. Global fitting for excited-state lifetime of BVE in solvents (TA)

	τ_1/ps	τ_2/ps	τ_3/ps	τ_4/ps
chloroform	-	1.6 ± 0.1	26 ± 4	-
acetonitrile	-	1.6 ± 0.1	25 ± 4	-
acetonitrile + water (V:V = 9:1)	0.81 ± 0.1	1.2 ± 0.1	5.7 ± 0.6	350 ± 30
methanol	0.84 ± 0.1	1.9 ± 0.1	38 ± 2	420 ± 10
deuterated methanol	0.85 ± 0.1	1.9 ± 0.1	40 ± 4	560 ± 20

Table S4. Best fitting for TA kinetics at 480 and 645 nm

	τ_1/ps	τ_2/ps	τ_3/ps	τ_4/ps
chloroform	-	1.6 ± 0.1 (95%)	26 ± 3 (5%)	-
acetonitrile	-	1.7 ± 0.1 (97%)	25 ± 3 (3%)	-
methanol	0.83 ± 0.10 (58%)	1.8 ± 0.2 (26%)	20 ± 5 (2%)	400 ± 10 (14%)

Table S5. Global fitting parameters of BVE TA data in chloroform mixtures [a]

$CHCl_3$ (1); $C_{10}H_{22}O_5$ (2). Viscosity at T = 298 K				
	χ_2	η /(mPa s) [b2]	τ_1 /ps	τ_2 /ps
$CHCl_3$	0.0000	0.532	1.6 ± 0.1	25 ± 1
Mixture 1	0.0600	0.810	1.6 ± 0.1	39 ± 3
Mixture 2	0.1180	1.124	1.6 ± 0.1	55 ± 4
Mixture 3	0.1876	1.492	1.6 ± 0.1	73 ± 8
Mixture 4	0.2957	2.04	1.6 ± 0.1	102 ± 10

[a] χ_2, the volume fraction of $C_{10}H_{22}O_5$ in total volume.

[b] parameters were taken from ref. 2

Reference

1. K. Ramamurthy, K. Ponnusamy and S. Chellappan, *RSC Advances*, 2020, **10**, 998-1006.
2. C. Wohlfarth, in *Landolt-börnstein - group iv physical chemistry* ed. M. D. Lechner, Springer-Verlag Berlin Heidelberg, 2008, vol. 25.